Hydrology and potential climate changes in the Rio Maipo (Chile)

ARTICLE *in* GEOGRAFIA FISICA E DINAMICCA QUATERNARIA · JANUARY 2015

Impact Factor: 0.63 · DOI: 10.4461/GFDQ.2015.38.14

8 AUTHORS, INCLUDING:


Andrea Soncini
Politecnico di Milano


Guglielmina Adele Diolaiuti
University of Milan


Claudio Smiraglia
University of Milan

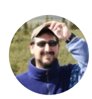
Daniele Bocchiola
Politecnico di Milano

Geogr. Fis. Dinam. Quat.
38 (2015), 155-168, 5 figg., 3 tab.

DOI 10.4461/GFDQ.2015.38.14

FLAVIO MIGLIAVACCA (*), GABRIELE CONFORTOLA(*), ANDREA SONCINI (*), ANTONELLA SENESE (**), GUGLIELMINA ADELE DIOLAIUTI (**), CLAUDIO SMIRAGLIA (**), GONZALO BARCAZA (***) & DANIELE BOCCHIOLA (*)

HYDROLOGY AND POTENTIAL CLIMATE CHANGES IN THE RIO MAIPO (CHILE)

ABSTRACT: MIGLIAVACCA F., CONFORTOLA G., SONCINI A., SENESE A., DIOLAIUTI G.A., SMIRAGLIA C., BARCAZA G. & BOCCHIOLA D, *Hydrology and potential climate changes in the Rio Maipo (Chile).* (IT ISSN 0391 – 9838, 2015)

Glaciers of the central Andes have recently been retreating in response to global warming, with large consequences on the hydrological regime. We assessed here potential climate change impacts until 2100 upon the hydrologic regime of the largely snow-ice melt driven Maipo River basin (closed at El Manzano, ca. 4800 km^2), watering 7 M people in the metropolitan region of Santiago de Chile. First, a weather-driven hydrological model including simplified glaciers' cover dynamics was set up and validated, to depict the hydrological regime of this area. In situ data from recent glaciological expeditions, ice thickness estimates, historical weather and hydrological data, and remote sensing data including precipitation from the Tropical Rainfall Measuring Mission (TRMM), and snow cover and temperature from the Moderate Resolution Imaging Spectroradiometer (MODIS) were used for model set up. We subsequently forced the model with projections of temperatures and precipitations (plus downscaling) until 2100 from the GCM model ECHAM6, according to 3 different radiative concentration pathways (RCPs 2.6, 4.5, 8.5) adopted by the IPCC in its AR5. We investigated yearly and seasonal trends of precipitation, temperature and hydrological fluxes until 2100 under the different scenarios, in projection period (PR, 2014-2100), and we compared them against historically observed trends in control period (CP, 1980-2013). The results show potential significant increasing trends in temperature until 2100, consistently with observed historical trends, unless for Spring (OND). Precipitation varies more uncertainly, with no historically significant changes, and only few scenarios projecting significant variations. In the PR period, yearly flow decreases, significantly under RCP8.5 (-0.31 m^{3}s^{-1}). Flow decrease is expected especially in Summer (JFM) under RCP8.5 (-0.55 m^{3}s^{-1}). Fall (AMJ) flows would decrease slightly, while winter (JAS) flows are projected to increase, and significantly under RCP4.5 (+0.22 m^{3}s^{-1}), as due to sustained melting therein. Spring (OND) flows also would decrease largely under RCP8.5, down to -0.67 m^{3}s^{-1}, due to increased evapotranspiration for high temperatures.

KEY WORDS**:** Climate change; Andes; Hydrological modeling; Remote sensing; Glaciers shrinkage.

RESUMEN: MIGLIAVACCA F., CONFORTOLA G., SONCINI A., SENESE A., DIOLAIUTI G.A., SMIRAGLIA C., BARCAZA G., BOCCHIOLA D, *Hidrologia y cambios climaticos potenciales nel rio Maipo (Chile)*. (IT ISSN 0391 – 9838, 2015)

Los glaciares de los Andes centrales se han recentemente derretido en respuesta al calientamento progresivo, con grandes consequencias sobre al regimen hidrologico. Aquì hemos estudiado los efectos potenciales del cambio climatico hasta al 2100 sobre al regimen hidrologico del riò Maipo (cerrado en El Manzano, ca. 4800 km^2), dependiente en largo sobra al derretimiento nivo-glacial y llevando aguas a 7 miliones de personas en la region de Santiago de Chile. Primero, un model hidrologico funcionante con datos de clima, y incluyendo la dinamica de glaciares, fue dasarrollado y validado para describir el regime hidrologico de esta area. Datos de campo tomados en campañas hidrologicas recentes, estimas de espesores de hielo, datos historicos de clima, datos hidrologicos y de sensores remotos incluyendo precipitationes de la misiòn TRMM y cubiertas de nieve de MODIS fueron usados para calibrar el modelo. Después el modelo fue adoprado con proyecciones de temperatura y precipitatión (con disagregación) hasta al 2100 del modelo GCM ECHAM6, segundo 3 diferentes historias de concentraciòn radiativa (RCPs 2.6, 4.5, 8.5) utilizadas por el IPCC en el AR5. Se investigaron las tendencias de precipitatión, temperatura y caudal hasta el 2100 bajo de los diferentes escenarios, and el periodo de proyeccion (PR, 2014-2100), y se las compararon encuentra las tendencias observadas en el periodo del control (CP, 1980-2013). Los resultados muestran tendencias potenciales de crecimiento de temperatura hasta el 2100, consistentes con los periodos historicos, si no per la Primavera Austral (OND). La precipita-

(*) *Dipartimento di Ingegneria Civile e Ambientale, Sezione Scienza e Ingegneria dell'Acqua (DICA-SIA), Politecnico di Milano, L. da Vinci 32, 20133, Milano, Italy.*

(**) *Dipartimento di Scienze della Terra "A. Desio", Università degli Studi di Milano, Mangiagalli 34, 20133, Milano, Italy."*

(***) *Dirección General de Aguas, Ministerio de Obras Pùblicas, Morandè 59, Santiago, Chile.*

The present work is in fulfilment of the project: "Cooperación técnica no reembolsable ATN/OC-11996 Chile, Programa plan de acción para la conservación de glaciares ante el cambio climático", Dirección General de Aguas, Ministerio de Obras Públicas, carried out during January-December 2012. Grant awarded to EVK2CNR, under scientific coordination of G. A. Diolaiuti. EVK2CNR, and most notably Dr. Luca Listo is kindly acknowledged for project's management, and logistic support. We acknowledge the World Climate Research Programme's Working Group on Coupled Modelling, which is responsible for CMIP and we thank the MPI-ESM for producing and making available their model outputs. The MODIS and TRMM data products are courtesy of the online Data Pool at the NASA Land Processes Distributed Active Archive Center (LP DAAC), USGS/Earth Resources Observation and Science (EROS) Center, Sioux Falls, South Dakota.

ción cambia con mas incertidumbre, no se registran cambios significativos y se encuentran muy pocos escenarios con cambios proyectados significativos. En el periodo PR, los caudales anuales disminuirán, significativamente bajo RCP8.5 (-0.31 $m^3s^{-1}y^{-1}$). La disminución se espera especialmente en el Verano Austral (JFM), bajo RCP8.5 (-0.55 $m^3s^{-1}y^{-1}$). Los caudales de Otoño (AMJ) disminuirán poco a poco, mientras que los caudales de Invierno (JAS) aumentarán, significativos bajo RCP4.5 (+0.22 $m^3s^{-1}y^{-1}$), debido al largo derretimiento. Los caudales primaverìl (OND) disminuirán en largo bajo RCP8.5, hasta -0.67 $m^3s^{-1}y^{-1}$, por la evapotraspiración debida a temperaturas altas.

Palabras Claves: Cambio Climatico; Andes; Modelos Hidrologicos; Sensores remotos; Derretimiento Glaciàl.

INTRODUCTION

Melt water from snow and ice within the Andes warrants water and food security of downstream populations. However, water security therein is at stake under demographic growth, changing climate (Urrutia & Vuille, 2009) and accelerated glaciers' shrinking (Rivera & alii, 2000; 2009; Bodin & alii, 2011; Pellicciotti & alii, 2008; 2011; 2014). Santiago and its metropolitan region (with more than 7 M inhabitants) depend largely upon water from the Maipo River, and 70% to 90% of the agricultural water comes from therein (Meza & *alii*, 2012), and also domestic use is expected to increase largely within this century (Ahumada & *alii*, 2013). The water in Central Chile rivers comes mainly from ice and snow melt, because the semi-arid climate therein displays mostly dry Summer and rain in Winter. Together with snow melt contribution, glaciers ensure runoff in arid seasons, with percentages that in the driest Summers may exceed 70-80%. In Chile, with the exception of the Patagonian region (18°-41° S), 1696 glaciers were inventoried, *i.e.* a total area of 1409 km^2, of which approximately 1000 km^2 in the central region (32°-36° S), with 1500 glaciers (Rivera & *alii*, 2000).

Global warming is affecting the Andes, with temperature rise, and negative effects upon mass balance of glaciers, and several studies showed that ice cover is shrinking dramatically. Since 1970 about 50% of the Andean cryosphere disappeared, against an average increase in temperature of +0.7° C (Rabatel & *alii*, 2011; 2013), less than that proposed by many climate change scenarios for the next decades. Rising of the isothermal 0° C accelerates melting of snow and ice, leading to an initial increase in discharge, but to a subsequent decrease in the long run. In the tropical Andes inversion is already happening, also due to decrease of solid precipitation (Carrasco & *alii*, 2005). The increasing temperatures also reduce the share of snow precipitation that would feed glaciers accumulation basins. The snowline already lifted in Central Chile by 127 metres on average during the last 25 years of the XX century (Masiokas & *alii*, 2009).

Recently Pelicciotti & *alii* (2014) reviewed recent status of glaciers and ice derived resources within the Andes of Chile. Briefly, they report that in the central Andes of Chile glaciers are shrinking, showing the examples of Juncal Norte, Juncal Sur, and Olivares Gamma glaciers, all close to (and the two latter nested into) the Maipo river catchment, loosing respectively -2.4%, -10.9%, and -8.2% in area, during 51 years since 1955 (Rivera & *alii*, 2002). However, glacier changes are not homogeneous, and local effects, including wind and gravitational redistribution seem to play an important role in determining glaciers' response. It is therefore clear why the response of the cryosphere to climate change is an issue of great interest to the scientific community, international organizations and policy makers (see *e.g.* National Climate Change Action Plan in Chile, National Environmental Commission, 2010). This study, in fulfilment of the project "Action plan for the safeguarding of the glaciers against climate change" for Chile, jointly carried out by Water General Division (Direccion General des Aguas, DGA) of Chile, and EvK2CNR association of Italy during 2012, aims at implementing and calibrating a hydrological model to simulate the present and future hydrological regime of the basin of Rio Maipo Alto (Upper Maipo river), using as inputs climate scenarios of the 5th Assessment Report (AR5) of the Intergovernmental Panel on Climate Change (IPCC, 2013). The largest complexity in tackling prospective hydrology of high altitude areas as here dwells into the gathering of field data, in harsh environmental conditions (see Bocchiola & *alii*, 2010, Soncini & *alii*, 2015). Here, to make up for the relative sparseness of weather and hydrological data, or malfunctioning at the highest altitudes, we complemented ground data using series of remote sensing data of precipitation (from Tropical Rainfall Measurement Mission TRMM), and temperature (from Moderate Resolution Imaging Spectroradiometer MODIS). The manuscript is structured as follows. i) First we describe the case study area, and data base including ground based data, remote sensing data, and climate projections from a GCM, ii) then we describe the methods adopted for hydro-glaciological modelling of the Maipo catchment, and projections until 2100, iii) we report the main results of our exercise, and finally iv) we provide a discussion including benchmarking against recent findings, and conclusions.

MAIPO RIVER

Our study covers the Maipo River Basin (Central Chile), closed at El Manzano (890 m a.s.l, 4839 km^2, Fig. 1), including the upper Maipo River and its main tributaries (Olivares, Colorado, Yeso and Volcàn). The basin is laid between 33°4' S and 34°15' S, and the altitude varies between 890 m a.s.l. of El Manzano to more than 6500 m a.s.l. of Tupungato. Hypsography displays 90% of the area above 2000 m a.s.l., and 60% above 3000 m a.s.l., including 364 km^2 of glaciers, or 8% of the area. The Rio Maipo (along with the Rio Mapocho) supplies largely the Santiago metropolitan region, with an average yearly (1980-2013) discharge of 120 m^3s^{-1}.

The soil is mostly bare (54%), with bushes (24%), and snowfields and glaciers (8%), and elsewhere forest, prairie, and steppe (MODIS land cover MCD12Q1, 500 m resolution). The area displays two different climatic regime (Peel & *alii*, 2007), namely i) temperate Mediterranean at low altitudes (below 2500 m a.s.l.), with a long dry season and clear separation between dry Summer and wet Winter (May to August, 95% of the annual precipitation), summer temperatures above 30°C, and strong thermal excursion, and ii) cold climate of high altitudes, with large winter snow

Fig. 1 - Case study. Rio Maipo. Weather and hydrologic stations, glaciers, and hypsometry. San Francisco and Pyramid Glaciers, where field campaigns were carried out in 2012.

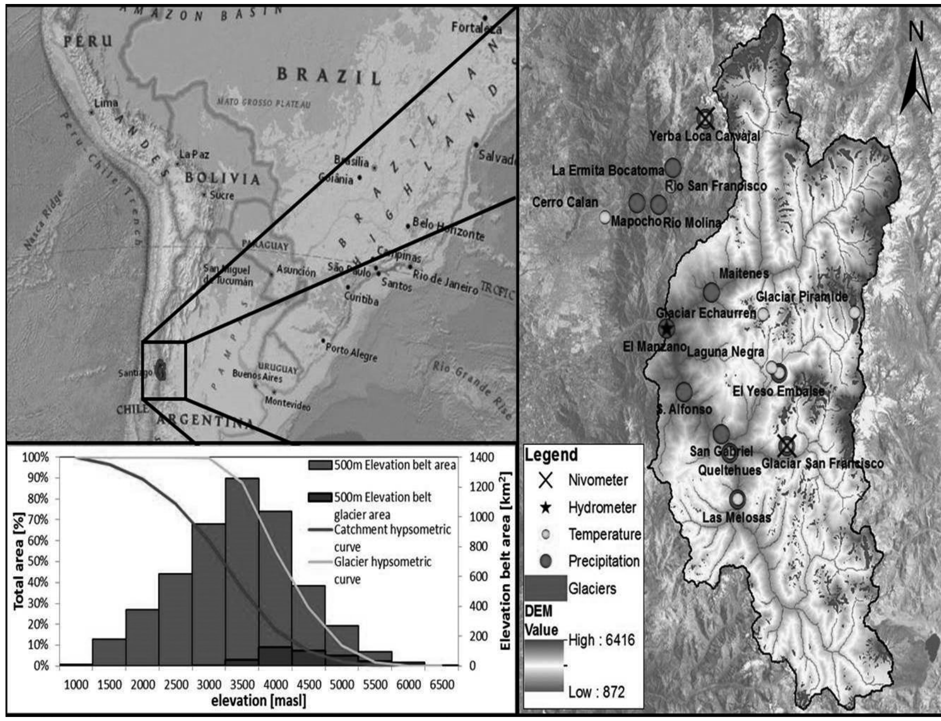

fall, and temperatures below 0°C. Rainfall tends to increase from North to South (Garreaud & Aceituno, 2001). El Niño oscillation has large effects in Central Chile, modifying precipitation, and temperature. Glaciers' mass balance during El Niño years may be positive due to larger precipitation (Masiokas & *alii*, 2006). Along the river, two main reservoirs are present, *i.e.* Laguna Negra (600 Mm^3) and el Yeso (250 Mm^3, closing the Yeso River).

HISTORICAL WEATHER AND HYDRO DATA

The hydrological model uses daily temperature and precipitation. We used data from 10 temperature stations, of which 7 are actually in the Maipo basin Rio Alto, and 3 are located northeast of Santiago (Rio Mapocho), close to the divide (fig. 1, Tab. 1). There are 12 available rainfall stations within Maipo, and nearby the catchment North of Santiago (fig. 1, Tab. 1). Rain gages are all located well below snow line, except for Yerba Loca Carvajal, which is not heated, and therefore not suitable for measurement in Winter. The measuring stations are property of the Direcciòn General de Aguas (with the exception of measures on the Pyramid Glacier, carried out by EvK2CNR technicians), and only 3 are higher than 3000 m a.s.l. Monthly lapse rates were taken from stations with at least 8 years of coverage. They vary from -6.9 °C km^{-1} to -5.2°C km^{-1}, in February and December. Precipitation lapse rates display increase at high altitudes. From 7 stations within the basin we found lapse rates from a minimum of +3 mm km^{-1} in December (Spring) to a maximum of +200 mm km^{-1} in July (Winter). The DGA made available daily flows (m^3s^{-1}) at the hydrometric station El Manzano (fig. 1), which we used here for model setup. In the Maipo catchment one snow depth gauging station is located near the San Francisco Glacier, at 2220 m a.s.l. (fig. 1). Also, we could use here the Yerba Loca Carvajal snow station, close to the divide at 3250 m a.s.l.

Table 1 - Weather and hydrometric stations available. Measured variables are temperature T, precipitation P, snow depth HS, discharge Q. See Figure 1 for position.

Station	Altitude [m a.s.l.]	Variable	Period available
Cerro Calan	848	T	(1975-2013)
Le Ermita Bocatoma	1350	T	(1987-2011)
Queltehues	1450	T, P	T(1987-2011), P(1972-1980)
Las Melosas	1527	T, P	T(1977-78), P(1962-2006)
Glaciar San Francisco	2220	T, P, HS	T(2012-2013), P(2012), HS(2012-2013)
El Yeso embalse	2475	T, P	T(1963-2013), P(1998-2013)
Laguna Negra	2780	T	T(2012-2013)
Yerba Loca Carvajal	3250	T,P, HS	T(2011-2013), P(2013), HS(2012-2013)
Glaciar Piramide	3587	T	T(March-April 2012)
Glaciar Echaurren	3850	T	T(1999-2001)
El Manzano	890	P, Q	P(2012-2013), Q(1695-2013)
Mapocho	966	P	(2012-13)
San Alfonso	1040	P	(1965-73, 2012-13)
Maitenes Bocatoma	1143	P	(1979-2013)
Rio Molina	1158	P	(2010-13)
San Gabriel	1266	P	(1977-2013)
Rio San Francisco	1550	P	April-July 2013

SATELLITE DATA

Given the relatively low coverage of the weather stations, especially at high altitudes, we decided to exploit satellite information to assess the spatial distribution of temperature and precipitation. Temperature data were taken from MOD11C3 product of MODIS (Moderate Resolution Imaging Spectroradiometer), on board of satellite Terra (EOS AM) for the even years during 2002-2012. To aid assessment of rainfall spatial distribution we used data from TRMM (Tropical Rainfall Measuring Mission, TRMM 2B31, Bookhagen & Burbank, 2006; 2010) during 1998-2009, with a resolution of 4x4 km^2, obtained by fusion of Precipitation Radar (PR) data, and TRMM Microwave Imager, on board of TRMM (see *e.g.* Bocchiola, 2007). Benchmarking of simulated snow cover on the ground by the model (and indirectly of snow water equivalent SWE daily value in each cell) was pursued using MOD10A2 product at 500 m resolution, 8 days composite (*e.g.* Parajka & *alii*, 2008a, b) during 2010-2012.

FIELD CAMPAIGNS

Field data were gathered during field campaigns carried out in 2012 by personnel of EvK2CNR under the project "Action plan for the safeguarding of the glaciers against climate change" of DGA (2012). These included, among others measurements upon 2 glaciers within the Maipo basin, *i.e.* San Francisco, and Pyramid. On the San Francisco Glacier, 7 ablation stakes were installed, covering 2890-3425 m a.s.l. Ablation was between 283 cm w.e. and 352 cm w.e. in 85 days (late January to late April 2012). Pyramid is a debris covered glacier, and supraglacial rock debris strongly modulates ice melt (Mihalcea & *alii*, 2006), then a melt factor was also assessed against debris thickness to predict ice ablation under a debris layer.

CLIMATE PROJECTIONS

A key to investigation of future hydrological conditions is the use of climate projections, properly tailored for the case study catchment. In the Fifth Assessment Report (AR5) by the Intergovernmental Panel on Climate Change IPCC a new set of scenarios describing four different Representative Concentration Pathways (RCPs, 2.6, 4.5, 6.5, 8.5) was presented (IPCC, 2013). Here, temperature and precipitation were used projected according to RCP2.6 (peak in radiative forcing at 3 Wm^{-2} or 490 ppm CO_2 equivalent in 2040, with decline to 2.6 Wm^{-2}), RCP4.5 (stabilization without overshoot pathway to 4.5 Wm^{-2}, or 650 ppm CO_2 eq. in 2070), and RCP8.5 (rising radiative forcing up to 8.5 Wm^{-2}, or 1370 ppm CO_2 eq. by 2100). Here the CCSM4 model was used (Gent & *alii*, 2011, https://www.earthsystemgrid.org). The coarse spatial resolution of GCMs may lead poor simulation of the effects of topography, *e.g.* precipitation changes over short distances, and in general spatial variability. Downscaling of the outputs of climate models is thus necessary to extract local information from coarse-scale simulations, and to perform hydrological studies at a basin scale (*e.g.* Groppelli & *alii*, 2011a).

GLACIO-HYDROLOGICAL MODELLING

A semi distributed, cell based hydrological model is used here, that was developed at Politecnico di Milano, usable to represent hydrological cycle of high altitude catchments (Groppelli & *alii*, 2011b; Bocchiola & *alii*, 2011; Confortola & *alii*, 2014; Soncini & *alii*, 2015). The model tracks the variation of the water content in the ground within one cell W [mm] in two consecutive time steps (t, $t+\Delta t$), as

$$W^{t+\Delta t} = W^t + R\Delta t + M_s\Delta t + M_i\Delta t - ET\Delta t - Q_g\Delta t, \quad (1)$$

Here using the daily time step R [mmd^{-1}] is the liquid rain, M_s [mmd^{-1}] is snowmelt, M_i [mmd^{-1}] is ice melt, ET [mmd^{-1}] is actual evapotranspiration, and Q_g [mmd^{-1}] is the groundwater discharge. Overland flow Q_s occurs for saturated soil

$$\begin{array}{lll} Q_s = W^{t+\Delta t} - W_{Max} & f & W^{t+\Delta t} > W_{Max} \\ Q_s = 0 & f & W^{t+\Delta t} \le W_{Max} \end{array}, \quad (2)$$

with W_{Max} [mm] greatest potential soil storage. Potential evapotranspiration is calculated via Hargreaves equation, requiring temperature data (see *e.g.* Bocchiola & *alii*, 2011). Groundwater discharge is a function of soil hydraulic conductivity and water content

$$Q_g = K\left(\frac{W}{W_{Max}}\right)^k, \quad (3)$$

with K [mmd^{-1}] saturated permeability and k [.] power exponent. Equations (1-3) are solved using a semi-distributed cell based scheme, different from the previously adopted altitude belt model (Groppelli & *alii*, 2011b; Bocchiola & *alii*, 2011), and originally adopted here. The model needs a DEM, daily precipitation and temperature, information of soil use, and vertical gradient of temperature and precipitation. Here we adapted to the cell based scheme a module specifically designed to take into account glacier flow as driven by gravity (see Soncini & *alii*, 2015). We approximated ice flow velocity by a simplified force balance, or proportional to shear stress raised to a power n, *i.e.* via Glen´s flow law ($n = 3$, *e.g.* Wallinga & van de Wal, 1998; Cuffey & Patterson, 2010). When basal shear stress τ_b [Pa] is either known or estimated, accounting for deformation and sliding velocity as governed by τ_b, one can approximate depth averaged ice velocity as (Oerlemans, 2001)

$$V_{ice,i} = K_d\tau_{b,i}^n h_{ice,i} + K_s\frac{\tau_{b,i}^n}{h_{ice,i}}, \quad (4)$$

with $h_{ice,i}$ [m] ice thickness in the cell i, and K_s [$m^{-3}\ y^{-1}$] and K_d [$m^{-1}\ y^{-1}$] parameters of basal sliding and internal deformation. Model calibration was carried out against observed flow velocities for the San Francisco and Piramide glaciers, where ice thickness was known, as estimated using GPR (see DGA, 2012). To initialize the ice flow model for catchment wide simulation, we had to estimate ice thickness $h_{ice.i}$ for each cell (with ice cover) within our catchment, to subsequently estimate basal shear τ_b therein as

$$\tau_{b,i} = \rho_i g h_{ice,i} \sin \alpha_i \ , \tag{5}$$

with ρ_i ice density [kg m^{-3}], g acceleration of gravity [9.8 m s^{-2}], and α_i local slope. DGA provided a shape file with estimated ice thickness at 2012 for all glaciers within the Maipo catchments. Avalanche nourishment on the glaciers is accounted for by considering the terrain slope. When ground slope is larger than a threshold, progressively more snow detaches (linearly increasing within 30°-60°), and falls in the nearest cell downstream, where it either melts, or transform into ice (see Soncini & *alii*, 2015). Once a year, 10% of snow at the end of the ablation season becomes new ice (*i.e.* ice formation takes 10 years). Flow discharges from each cell are routed to outlet using a semi-distributed flow routing algorithm, based upon instantaneous unit hydrograph, IUH (*e.g.* Rosso, 1984). The model has two (parallel) systems (groundwater, overland), each one with a given number of reservoirs in series (n_g and n_s). Each reservoir possesses a time constant (*i.e.* k_g, k_s), or lag time, proportional to hydraulic path to the outlet section. The grid size adopted here was 3x3 km^2. This is somewhat large considering the characteristic size of glaciers within the catchment (the largest glacier being Juncal Sur, covering with 21 km^2 ca., DGA, 2011). However, given the size of Maipo catchment here, this size allowed a reasonable trade-off between accuracy of depiction of the distributed processes including ice flow, and computational burden for simulation at the catchment scale, and for long term simulation of climate change effects under several scenarios.

TEMPERATURE AND PRECIPITATION CORRECTION USING SATELLITE DATA

We used monthly averages of temperature from the ground stations to assess a monthly lapse rate for temperature extrapolation at high altitudes. Also, we evaluated monthly average temperatures, and lapse rates from MOD11C3 data in the same cells (3x3 km^2) including the temperatures gages. In spite of some overestimation, MOD11C3 gave a lapse rate very close to that from ground stations (-5.3°C km^{-1} against -5.8°C km^{-1} yearly), for all months (not shown), and for higher altitudes than with the ground stations (*i.e.* until 5700 m a.s.l. using MOD11C3 *vs* 3600 using ground stations). Accordingly, we could use MOD11C3 to provide spatial distribution of temperature for better distributed modelling (Barros & *alii*, 2002). To do so, we calculated for each cell of the catchment (3x3 km^2) the average yearly temperature from the MOD11C3 maps. By comparing the temperature in each cell of the so obtained temperature grid against the potential temperature (*i.e.* calculated at the same altitude) from ground based lapse rates, we obtained a distributed maps of additive temperature corrections to be applied to obtain distributed temperature fields. We initially did so on a monthly basis, but it turned out that no significant difference was seen, nor hydrological modelling would profit from this, so correction was applied using yearly average corrections. Also, to aid assessment of rainfall spatial distribution we used data from TRMM (Tropical Rainfall Measuring Mission, TRMM 2B31, Bookhagen & Burbank, 2006). Monthly average TRMM rainfall was estimated within the same cells (3x3 km^2) including the rainfall gages. This provided acceptable agreement (*i.e.* accurate depiction of precipitation lapse rates) only at low altitudes (*i.e.* below 2500 m a.s.l., not shown), due to occurrence of snowfall, badly detected by TRMM. We thus decided to apply TRMM correction only in Summer (JFM), when no snowfall occurs generally. Similarly to temperature, we calculated for each cell of the catchment (3x3 km^2) the summer mean rainfall from TRMM data. By comparing rainfall in each cell of the so obtained rainfall grid against the potential rainfall (*i.e.* calculated at the same altitude) from ground based lapse rates, we obtained distributed maps of rainfall (multiplicative) correction to be applied to obtain distributed rainfall fields. During any other season, precipitation was distributed according to monthly lapse rates as from ground stations with a considerably long data series, placed at altitudes normally not affected by large snowfalls.

SNOW AND ICE ABLATION MODELLING

Snow melt M_s was estimated here using degree day approach

$$M_s = D_D \ (T\text{-}T_t) \ , \tag{6}$$

with T daily mean temperature, D_D snow melt factor [mm°C^{-1}d^{-1}], and T_t threshold temperature (*e.g.* Bocchiola & *alii*, 2010). Local snow melt factors were estimated from snow data at Yerba Loca station (year 2013), and at San Francisco glacier (2012). Similar values were found therein, namely D_D = 5.9 mm°C^{-1}d^{-1} for Yerba Loca, and D_D = 6.5 mm°C^{-1}d^{-1} for San Francisco. A constant threshold T_t = -1°C (Haby, 2008) for Degree-Day was taken, after data analysis. However, being these values site-specific, they could not be seen as representative of all glaciers in the basin, and D_D was used as a parameter for model tuning, with the assumption its value would not differ too much from those reported here. Similarly ice melt M_i was estimated using a degree day

$$M_i = D_I \ (T\text{-}T_t) \ , \tag{7}$$

with D_I ice melt factor [mm°C^{-1}d^{-1}]. Analysis of ice ablation data from 7 stakes upon the San Francisco glacier, displaying bare ice, yielded a somewhat constant (with altitude, from 2890 m a.s.l. to 3425 m a.s.l.) value of D_I = 4.1 mm°C^{-1}d^{-1} (see DGA, 2012). Pyramid glacier is instead a debris covered glacier. From ablation at 4 stakes displaying variable debris cover thickness (ca. 5 to 50 cm) gathered in 2012 (see DGA, 2012), we calculated values of D_I ranging from a largest D_I = 4.5 mm°C^{-1}d^{-1} at 10 cm, to D_I = 2.5 mm°C^{-1}d^{-1} at 25 cm, to an estimated D_I = 2.6 mm°C^{-1}d^{-1} at 0 cm (bare ice), values that are not very large, since in the literature melt factor may reach up to 20 mm°C^{-1}d^{-1} (Hock, 2003). Again, such values are site specific, and cannot in principle be extended to other glaciers. Notice further that accurate debris cover mapping is not available for the Maipo river that we know of, unless locally (*e.g.* Laguna negra, Bodin & *alii*, 2010). A rough estimation of debris cover carried by the authors here within the Maipo catchment glaciers would indicate 45% or so of area cover (DGA, 2011), but accurate assessment requires effort beyond the present manuscript (see. *e.g.* Minora & *alii*, 2013). However, even with debris cover area known, accurate ice melt assessment under debris requires site specific ablation data, and spatially distributed debris thickness mapping (see *e.g.* Bocchiola & *alii*, 2010; Soncini & *alii*, 2015). Accordingly, it seems not possible here i) to accurately assess debris cover area, and thickness, ii) to accurately estimate ice ablation on each either bare, or debris covered glacier. As a result of these reasonings, again here we decided to use D_I as a parameter for model tuning, with the assumption its value would not differ too much from those reported from the mentioned field studies (as done *e.g.* in Bocchiola & *alii*, 2011).

DOWNSCALING OF GCM PROJECTIONS

To tailor climate scenarios from *GCMs* for our region of interest, we pursued statistical downscaling. For precipitation, disaggregation was carried out using the theory of stochastic time random cascade, SSRC (*e.g.* Groppelli & *alii*, 2011a). The SSRC was tuned using the 1994-2003 daily series of precipitation at S. Gabriel station, the most complete one. The downscaling approach using SSRC first corrects the daily precipitation bias. A constant (multiplicative) term is used to force the average daily value of precipitation from the GCM to equate its observed value. In addition a β model (binomial) generator is used to evaluate the probability of wet (or dry) spells to reproduce intermittence. Finally a "strictly positive" generator added a proper amount of variability to precipitation during spells labelled as wet. Model estimation of SSRC is explained elsewhere (Groppelli & *alii*, 2011a) and the reader is addressed therein. The estimated parameters were then used to disaggregate the future precipitation projected under the three RCP scenarios. Temperature downscaling was also carried out, using the 1994-2003 temperature series in Yeso Embalse station. A monthly *Delta-T* approach was used to project the temperature values (Groppelli & *alii*, 2011b). After downscaling, both precipitation and temperature were corrected for altitude using lapse rates, and further spatial distribution was modeled as reported in Section 3.2. Eventually, we obtained series of spatially distributed daily projected precipitation and temperature for each RCP, to be fed to the hydrological model for future water resources projections.

TREND ANALYSIS

Given that we had available weather (temperature, since 1981, precipitation since 1982), and hydrological (since 1980) series for at least one station in the catchment, we decided to perform trend analysis (using linear regression LR) on each of these variables for the available period in the past, which we call CP, to verify the presence of any measurable change. We evaluated yearly, and seasonal trends of temperature (Yeso Embalse), precipitation (San Gabriel), and flow discharge (El Manzano). Also, we estimated the projected climate and hydrologic trends in the same stations as from our three scenarios during the projections period PR (2014-2100). Albeit more complex and accurate methods exist to assess non stationarity of climate series, maybe combining more tests (*e.g.* Bocchiola & Diolaiuti, 2013), here the purpose is to evaluate the magnitude, and possibly significance, of linear variation in time of climate, and especially water resources for planning purposes, and investigate whether future climate evolution may change (*i.e.* either increase or decrease) against recently observed trends.

MODELS' PERFORMANCE

In Figure 2 we report model calibration (1994-2003) *vs* observed discharges at El Manzano station. In Table 2, we report calibration, and validation statistics (validation not shown, qualitatively similar to Figure 2). Also in Figure 2 we report daily contribution to runoff from precipitation, and snow and ice melt as simulated by the model, to highlight flow generation mechanism. In Table 2 we also reported best statistics for calibration (and subsequent validation) obtained without correction of ground temperature, and of rainfall using remote sensing (NSE_{NS}, $RMSE_{NS}$), and with only use of TRMM rainfall data (no temperature correction, NSE_{TR}, $RMSE_{TR}$). Comparison with validation statistics above (and visual analysis not shown) demonstrated that use of spatially corrected precipitation, and temperature may provide some improvement to hydrological modelling exercise. Also in Table 2 we report seasonal validation statistics, namely seasonal average flow values, to investigate seasonal matching of the model, including different flow generating mechanism (*i.e.* mostly snow melt during Spring OND, mostly ice melt during Summer JFM, mixed during Fall, AMJ and Winter JAS (fig. 2). Generally, the model well represents on average seasonal flow dynamics. Snow degree day was set to D_D = 5.6 mm°C^{-1}d^{-1}, pretty close to those as estimated from snow data, as reported in Section 3.3 (D_D = 5.9 mm°C^{-1}d^{-1} for Yerba Loca, and D_D = 6.5 mm°C^{-1}d^{-1} for San Francisco). Average monthly snow cover during Winter and Spring (JAS, OND, where most of the dynamics of snow accumulation and depletion is played) simulated from the model during 2010-2012 was benchmarked *vs* the same variable, as derived using MOD10A2, *i.e.* 8 days composite at 500 m resolution, with acceptable results (not shown), witnessing good capability of the model to capture snow dynamics. Ice degree day was set during calibration to D_D = 7.2 mm°C^{-1}d^{-1}, larger than those observed upon our case study glaciers (D_I = 4.1 mm°C^{-1}d^{-1} for San Francisco, D_I = 2.6-4.5 mm°C^{-1}d^{-1} on Pyramid Glacier, depending on debris cover), but still in line with expected values in literature (see *e.g.* Singh & *alii*, 2000, Hock, 1999; 2003). As reported in Section 3.3, our measured values covered two only glaciers during Summer 2012, and may not be spatially (*e.g.* for latitude, exposition, etc..), and temporally representative. Also as reported, no spatially distributed information is available of debris cover properties in the catchment's glaciers, so the D_I value from calibration is used as a representative value for the glaciers in the area. This may be not accurate enough to depict small scale glaciers' dynamics, but instead seems sufficient to depict present, and future large scale ice ablation and hydrological dynamics. In Figure 2 the modeled specific contribution is also reported [mmd^{-1}] from snow melt q_s, ice melt q_i, and rainfall q_r ($q = q_s + q_i + q_r$), to provide an indication of flow generation regime in different periods. Therein it is clearly visible the large increase in discharge during Spring (OND) as due to snow melt, and subsequently increasing flows in Summer (JFM), occurring at the expenses of ice melt, when snow cover is mostly depleted, with noticeable ice melt contribution during Fall (AMJ). Rainfall only sporadically contributes to flow, mostly during Winter (JAS). On a yearly average during 1994-2003 the model provided E[q_s] = 1.26 mmd^{-1}, E[q_i] = 0.33 mmd^{-1}, E[q_r] = 0.10 mmd^{-1}, *i.e.* with snow melt contribution threefold of ice melt, and tenfold of rainfall.

TABLE 2 - Glacio-hydrological model parameters after calibration (1994-2003), and goodness of fit (calibration, and validation, 2008-2011). Parameter with values in *Italic* indicates values from literature, or coming from *a priori* analysis of topography, land cover, etc. Also, method of estimation explained. Goodness of fit measures reported, including method of estimation when using a specific measure for calibration (*e.g.* minimization of *Bias*, maximization of *NSE*, etc..). We also report yearly and seasonal flow statistic, observed and modelled. Seasonal flows are reported with confidence limits (±95%) to provide goodness of fit assessment.

Parameter	Description	Value	Method
		Calibration	
W_{max} [mm]	Max soil water content (average)	244	Land use analysis
D_D [mm°C^{-1}d^{-1}]	Snow Degree Day	5.6	Snow data/valid *vs* MODIS
D_I [mm°C^{-1}d^{-1}]	Ice Degree Day	7.2	Surveys/Calibration *vs* flow
k [.]	Groundwater flow exponent	2	Max NSE, Bias correction
K [mmd^{-1}]	Hydraulic conductivity	4	Max NSE, Bias correction
t_s [d]	Lag time surface	3	Max NSE, high flows
t_g [d]	Lag time subsurface	20	Max NSE, low flows
n [.]	Number of reservoir (sup./subsup.)	4/5	Literature
K_d[m^{-1}y^{-1}]	Ice flow deformation coefficient	0.98E^{-16}	Ice stakes (SF, PI)/Literature
K_s[m^{-3}y^{-1}]	Ice flow basal sliding coefficient	1E^{-14}	Ice stakes (SF, PI)/Literature
		Goodness of fit (Calib,Valid.)	
Bias [%]	Daily average percentage error	-4.4,-4.7	Minimization (for Calib.)
NSE [.]	Daily Nash Sutcliffe efficiency	0.81,0.79	Maximization (for Calib.)
RMSE [m^{3}s^{-1}]	Daily Random mean square error	24.2,17.2	-
RMSE [%]	Percentage RMSE	23,19	-
NSE_{NS} [.]	*NSE* without satellite correction	0.62, 0.61	Maximization (for Calib.)
$RMSE_{NS}$ [m^{3}s^{-1}]	*RMSE* without satellite correction	35.0, 23.53	-
NSE_{TR} [.]	*NSE* using only TRMM	0.77, 0.74	Maximization (for Calib.)
$RMSE_{TR}$ [m^{3}s^{-1}]	*RMSE* using only TRMM	26.5, 19.5	-
$Bias_I$ [%]	Percentage error ice flow vel.	-4	Minimization (for Calib.)
R^2_I [.]	Det. Coefficient ice flow vel	0.56	Maximization (for Calib.)
		Flow statistics obs/mod (Calib.,Valid.)	
Q_{av} [m^{3}s^{-1}]	Average flow discharge (±95%)	113±3/108, 94±3/89	Best fitting (for Calib.)
σ_Q [m^{3}s^{-1}]	Standard deviation of flow discharge	84/83, 59/60	-
CV_Q[.]	Coeff. of variation of flow discharge	0.75/0.76	-
Q_{avY} [m^{3}s^{-1}]	Av. stream flow yearly (±95%)	113±17.1/108, 93±16/89	
Q_{avJFM} [m^{3}s^{-1}]	Av. stream flow JFM (±95%)	156±43/155, 121±21/125	-
Q_{avAMJ} [m^{3}s^{-1}]	Av. stream flow AMJ (±95%)	65±8/73, 64±10/66	-
Q_{avJAS} [m^{3}s^{-1}]	Av. stream flow JAS (±95%)	68±12/62, 58±10/46	-
Q_{avOND} [m^{3}s^{-1}]	Av. stream flow OND (±95%)	163±40/142, 130±30/119	-

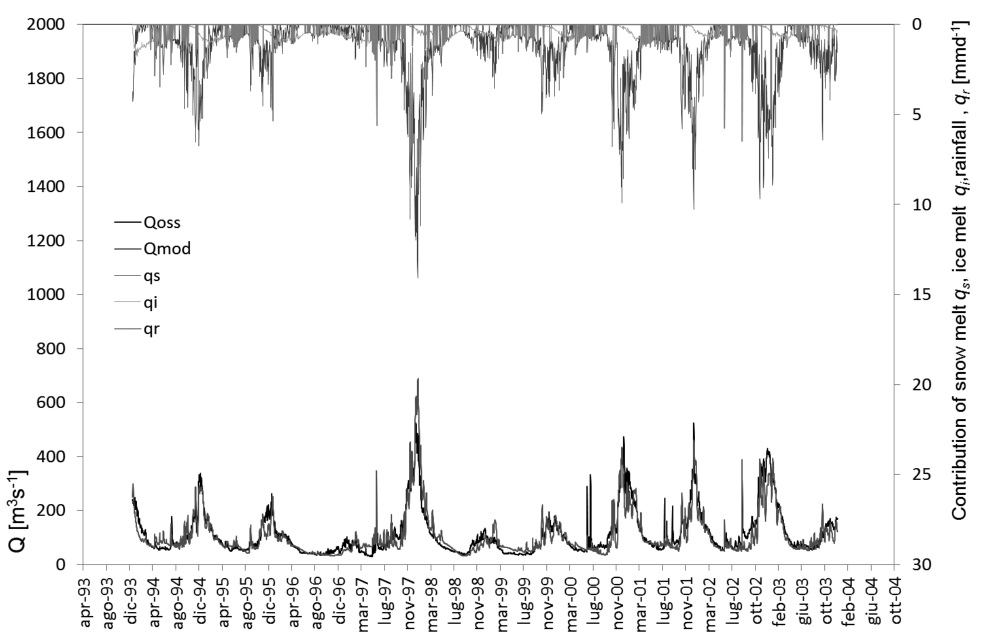

FIG. 2 - Rio Maipo at El Manzano. Daily observed and modelled discharges for Model calibration (1994-2013). Specific contribution [mmd^{-1}] reported, from snow melt q_s, ice melt qi, rainfall q_r.

ICE FLOW MODEL PERFORMANCE

Ice flow model calibration is reported in Figure 3. Therein, flow velocity (observed) is reported against basal shear stress, as estimated from measured ice thickness (DGA, 2012), separately for San Francisco, and Pyramid glacier. Also, interpolation as obtained using Eq. (4) properly tuned *vs* the observations. Visibly, a good fitting is reported, also considering that two different glaciers are modelled. Pyramid glacier is ca. 20 km more northern than San Francisco glacier, and they are both predominantly exposed southward. However, Pyramid glacier stretches for ca. 8 km in length, with an altitude range from ca. 3200 m a.s.l. to ca. 4000 m a.s.l., and average slope of 10%. In the three measured sites (*i.e.* for stake velocity), average slope range is 11%, with average measured velocity of 9.6 my^{-1}. San Francisco glacier spans a wider altitude range (ca. 2700-4000 m a.s.l.), and it is shorter (ca. 3 km) and much steeper, and the average slope in the six measured (*i.e.* for stake velocity) sites was 30%, with an average velocity of 16 my^{-1}. Accordingly, the capability of the model to reproduce acceptably the velocity field for both glaciers seems to indicate an acceptable depiction of ice flow velocity in the area. In Table 2, goodness of fit is reported. A *Bias* = -4% is observed, with a determination coefficient R_I^2 = 0.56. Given the seemingly acceptable performance of the ice flow model, we could use it for description of ice flow within all glaciers in the area, for the purpose of large scale assessment of ice cover dynamics for hydrological modelling, and projections.

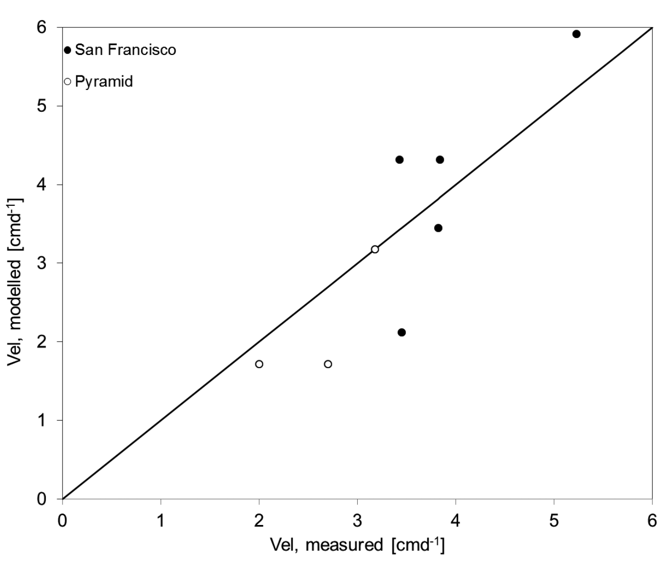

FIG. 3 - Ice flow model calibration. Measured and modelled velocity on San Francisco and Pyramid glaciers (Summer 2012).

HYDROLOGICAL PROJECTIONS AND TRENDS UNTIL 2100

Seasonal hydrological projections are reported in Figure 4, together with their CP (1980-2013) counterpart. During Summer (JFM, fig. 4a) mostly flow decrease is seen under all RCPs. Fall (AMJ, fig. 4b), and Winter (JAS, fig. 4c) display visible decrease in CP, and increase in PR, and Spring (OND, fig. 4d) shows decrease on CP, and substantial stationarity during PR on average. Again, seasonal trends of stream flows under all scenarios were investigated in depth, reported in Table 3.

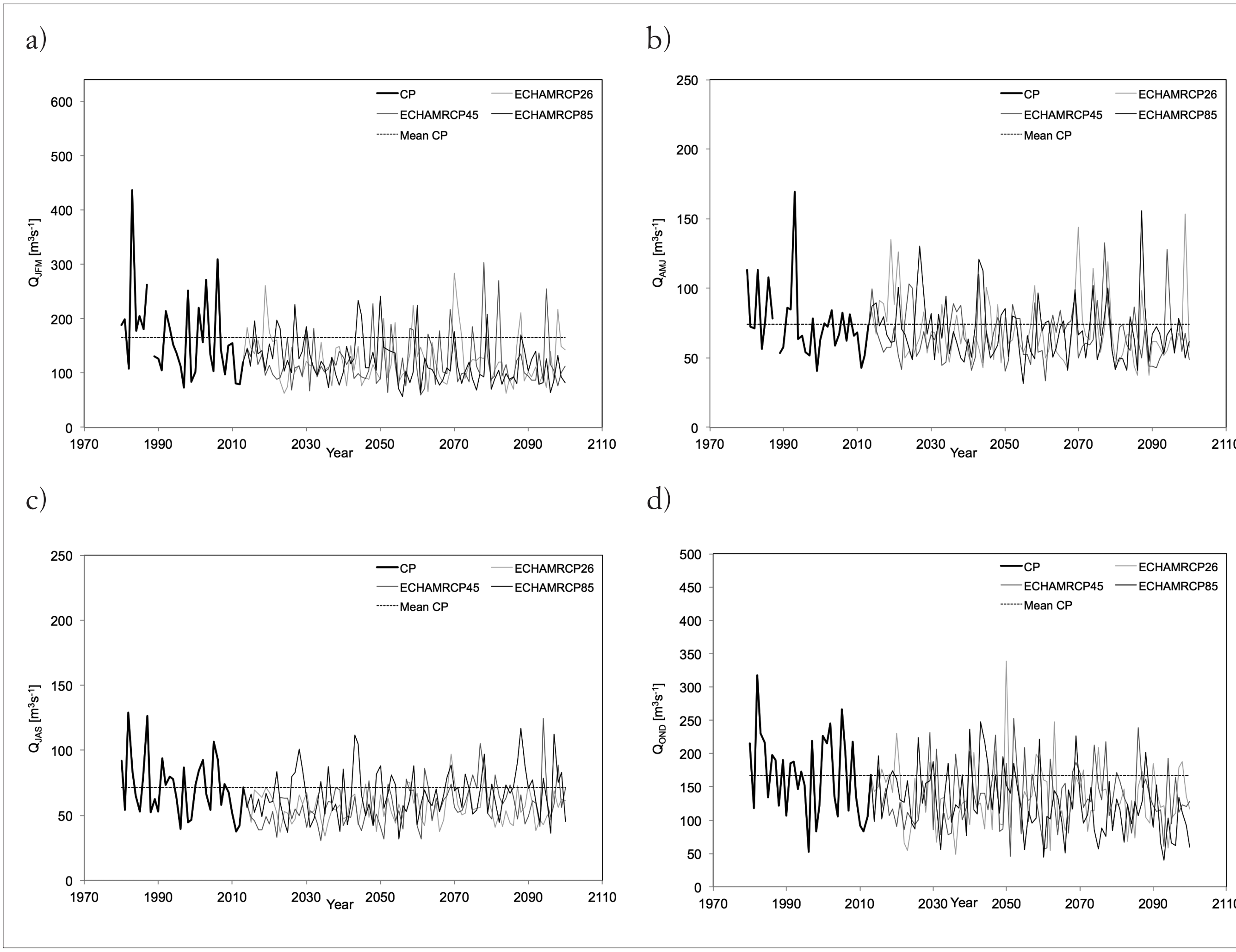

FIG. 4 - Rio Maipo at El Manzano. Stream flow projections until 2100 vs CP (1980-2014). a) Year a) Summer JFM. b) Fall AMJ. c) Winter JAS. D) Spring OND.

We here quantified climate and hydrological trends using linear regression LR as from two periods, namely CP (1980/1/2-2013, for discharge, temperature and precipitation), and PR (2014-2100), to highlight yearly and seasonal changes in the area under past and future climate change, and benchmark our projections against past observed trends. In Table 3 we report seasonal indicators, including regression slope, and indication of significance (α = 5%, bold values). In Figure 5 we resume trends for climate and hydrology for PR as per RCPs, regardless of their significance (see Tab. 3). Temperature in Table 3 always increases during PR (and always significantly for RCP4.5 and RCP8.5), unless for a slight decrease in Winter (JAS) under RCP2.6. RCP2.6 depicts large increase of temperature initially (starting since 2014 and until half century), followed optimistically by large attempt for mitigation of global warming, and accordingly temperature may decrease therein at the end of the century. Precipitation during CP decreased yearly, and during Winter JAS, and Spring OND, but variations were never significant. Projected values during PR are occasionally increasing or decreasing, but not clear patterns are visible. However, under RCP8.5, total (yearly), and Winter JAS precipitation decreases significantly. From Table 3, at the Y scale decrease of mean flows (-1.5 $m^3s^{-1}y^{-1}$) is observed during CP (1980-2013), statistically significant. From Figure 5, RCP2.6 and RCP8.5 provide decreasing yearly flows, and significantly for RCP8.5, with largest decrease projected at -0.31 $m^3s^{-1}y^{-1}$ until 2100. This in spite of RCP4.5 projecting very slightly increasing Q during PR. The largest flow changes are projected during Summer, JFM under RCP8.5. During CP large significant flow decrease was detected (down to -2.6 $m^3s^{-1}y^{-1}$) in Summer, so such trend may continue in the future for largely increasing temperature under RCP8.5. During Fall AMJ, all RCPs provide not significant decrease. In Winter JAS significant increase is projected under RCP4.5 (+0.22 $m^3s^{-1}y^{-1}$). During Spring OND, a somewhat large flow decrease is projected under RCP8.5 (-0.67 $m^3s^{-1}y^{-1}$).

TABLE 3 - Climate and hydrological trends, CP, and PR periods. For CP periods, average values reported. In bold significant values (α = 5%).

		Season	P, CP	T, CP	Q, CP
	CP	Year	-2.4E-02	2.0E-02	**-1.5E+00**
	CP	JFM	3.3E-03	**2.5E-02**	**-2.6E+00**
	CP	AMJ	1.7E-02	**4.6E-02**	-7.8E-01
	CP	JAS	-6.5E-02	1.3E-02	-6.5E-01
	CP	OND	-9.3E-04	-3.8E-03	-1.7E+00
Scenario		**Season**	**P, PR**	**T, PR**	**Q, PR**
ECHAMRCP26		Year	3.3E-03	1.4E-03	-9.9E-02
ECHAMRCP26		JFM	1.0E-03	3.8E-03	-1.4E-01
ECHAMRCP26		AMJ	-2.9E-03	1.9E-03	-1.1E-01
ECHAMRCP26		JAS	1.3E-02	-1.5E-03	-2.1E-02
ECHAMRCP26		OND	1.7E-03	1.3E-03	-1.3E-01
ECHAMRCP45		Year	-2.0E-04	**1.6E-02**	1.0E-01
ECHAMRCP45		JFM	-9.4E-04	**1.7E-02**	7.0E-02
ECHAMRCP45		AMJ	3.0E-03	**1.5E-02**	-2.5E-02
ECHAMRCP45		JAS	-6.8E-03	**1.8E-02**	**2.2E-01**
ECHAMRCP45		OND	4.4E-03	**1.5E-02**	1.4E-01
ECHAMRCP85		Year	**-6.6E-03**	**4.9E-02**	**-3.1E-01**
ECHAMRCP85		JFM	-9.2E-04	**5.5E-02**	**-5.5E-01**
ECHAMRCP85		AMJ	-8.2E-03	**4.6E-02**	-1.2E-01
ECHAMRCP85		JAS	**-1.7E-02**	**4.6E-02**	1.0E-01
ECHAMRCP85		OND	-3.1E-04	**4.9E-02**	**-6.7E-01**

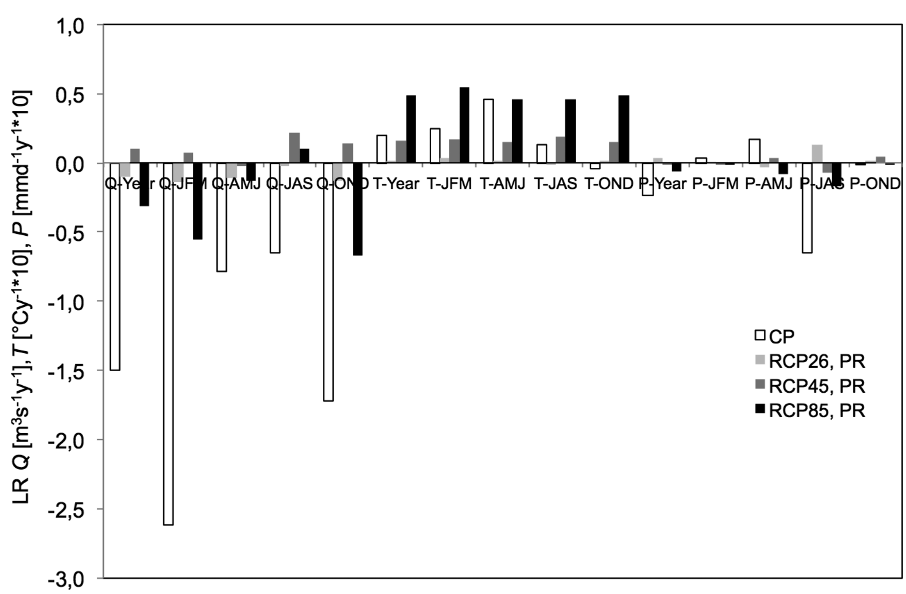

FIG. 5 - Projected trends of discharge yearly and seasonal discharge Q, precipitation P, temperature T until 2100 as per RCPs vs CP period.

DISCUSSION AND CONCLUSIONS

Our glacio-hydrological model provides a seemingly accurate depiction of stream flows in to the Maipo River. Daily flows and their variability in response to weather patterns seem well depicted. Also, seasonal flow regimes are well depicted both in calibration, and validation phase, witnessing acceptable capacity of the model to capture seasonal response to climate variability. Accordingly, one can reasonably rely upon use of the model to project forward in time the catchment response to future climate trends, in the hypothesis that physical response patterns of the catchment (*i.e.* tuned parameters such as degree-days, physical landscape of soil cover and use, etc..) would not change largely in the future. During Summer, flow decrease is substantially projected to decrease in the future, so continuing the observed significant trends of the recent past (CP period, Tab. 3, fig. 5). Analysis of snow and ice melt, and evapotranspiration (not shown) displayed that the projected decrease of Q during JFM is likely to be charged to decreased ice melt during PR period, and especially under RCP8.5. Initially in PR period increasing ice melt is projected, ad due to increasing temperature, but with subsequent decrease, especially under RCP2.6 and RCP4.5. Accordingly, stream flows during JFM largely depends upon snow and ice melt, but the latter decreases with time. Also increasing *ET* as driven by high temperatures especially under RCP8.5 may further decrease flow discharge. In Fall AMJ the same trends as in JFM persist. Ice melt is still sustained in Fall (fig. 2), and decreasing ice melt starting from the 90s' (not shown) may have reduced Q in the CP period. Also, slightly increasing *ET* (as due to significantly increasing T, Tab. 3) may have further affected flow decrease. In the PR period, sustained melting from higher temperatures would maintain stream flow at the present level during Fall for most of the century. During Winter significant increase of stream flow was detected under RCP4.5. Stream flows slightly decreased during CP, possibly due to decreased precipitation (Tab. 3). During PR, both ice and snow melt would increase due to increasing T, with rainfall substantially constant. Increasing *ET* in response to increasing T would not be able to offset increased melting, and accordingly Winter stream flows would increase at the end of the century. In Spring OND historically discharge decreased visibly (albeit not significantly, Table 3, *p-val* = 0.09), in spite of substantially constant T, and P. Analysis of ice melt during Spring (not shown) displays decreasing values during CP, consistently with ice volume decreasing, which together with substantially constant snow melt may explain decreasing Q. At the yearly scale, projected trends for the future would be consistent with past observations. During CP, significant flow decrease has been detected, given possibly by decreasing ice cover since the 90s, and possibly increasing evapotranspiration. The projected trends indicate substantially constant, or slightly decreasing flows as given by trading off of initial increased ice melting, followed by decreasing ice availability, and increasing evapotranspiration, especially under RCP8.5.

Eventually, the projected scenarios consistently indicate a potential evolution of the hydrology of the Maipo river as dominated by temperature increase, with the twofold effects of increasing ice and snow melt (the latter being faster, but substantially constant at the yearly scale given slight changes in precipitation), and changing ice volume availability, initially larger given rise of the temperature (and altitude of the melting area), but lately smaller for depletion. On average (on the three RCPs), at the end of the century, yearly mean discharge would change from 120 m^3s^{-1} now (1980-2013), to 92 m^3s^{-1} (-23%) at the end of the century (2071-2100), with a variability between 86 m^3s^{-1} and 99 m^3s^{-1} (-28% to -18%).

Few contributions are available in the present literature concerning future potential hydrology within the Chilean Andes and the Maipo catchment, against which we can benchmark our findings. Among others, Pellicciotti & *alii* (2014) presented a climate change study upon the Juncal Norte Glacier, North of our Maipo catchment here. Using climate scenarios from 2 GCMs (ECHAM5, HadCM3) included within the CMIP3 experiment (AR4 of IPCC), and storyline A1B (medium optimistic) they projected mass balance of the glacier until 2050, and water production including rainfall, and melt in the Juncal Norte catchment. At the yearly scale, they projected a decrease of runoff down to -30% or so under HadCM3, with substantially constant runoff under ECHAM5 (Pellicciotti & *alii*, 2014, see fig. 8). Our projections until 2050 (fig. 4) depict (decade 2045-2054) a change in runoff (*vs* 1980-2013) ranging from -21% (RCP4.5) to -10% (RCP8.5). However, the model by Pellicciotti & *alii* (2014) would not include ice flow, so making mass balance and hydrological projections biased, because snow and ice at high altitudes are unable to move downwards, making accumulation at those altitude unreasonable (see also Bocchiola & *alii*, 2011), and rapidly down wasting ablation tongues, so changing runoff patterns. Also, they do not include evapotranspiration in their calculation of runoff, which is indeed influencing water budget, especially under the hottest RCP8.5 scenarios. Our results here provide an improvement in this sense. Ahumada & *alii* (2013) studied potential effects of climate change until 2065 upon water availability in the Maipo River, closed at El Manzano. Based on a previous study within Maipo River (CEPAL, 2009), and upon regression analysis, they projected monthly flow discharge at El Manzano during 2035-2065, and estimated a -12% drop yearly, similarly to here (-22% with RCP4.5 to -18% with RCP8.5). However, apparently no physically based modelling was pursued by Ahumada & *alii* (2013) to explain the physical patterns behind such changes. Meza & *alii* (2012) studied potential impacts of climate change on irrigated agriculture in the Maipo basin. They used a multisite stochastic weather generator able to downscale A2 and B2 emission scenarios from GCM, and a hydrological model including crop production, to generate monthly flows of the Maipo River at El Manzano during 2071-2100. They found that during irrigation season in Spring and Summer (OND+JFM) large flow decrease would occur, and that the 15th percentile (*i.e.* with 15% probability of failure) currently used as the basis for water rights allocation, may become the 40th or 50th percentile (*i.e.* irrigation demand would be unmet in 40%, or 50% of the cases, B2, and A2 scenario, respectively) in the future, suggesting that water allocation for future irrigation will be unsustainable at the present levels. Albeit we did not focus here upon irrigation demands, our estimates for 2071-2100 during irrigation season ranges from -38% (RCP8.5) to -22% (RCP4.5) *vs* CP, clearly upholding the findings from Meza & *alii* (2012). Krellenberg & Hansjürgens (2014) investigated the effects of climate change in the metropolitan region of Santiago. Based on Cortés & *alii* (2012) they addressed water availability in the Maipo River (El Manzano) based upon AR5 climate projections, projecting a potential decrease of runoff until 2050 from -19% (B1 storyline) to -30% (A2 storyline), somewhat larger than here (from -21% with RCP4.5 to -10% with RCP8.5). According to what reported here, our results provide an approach that is updated (*i.e.* based upon more recently developed climate projections within AR5 of IPCC), and physically based (*i.e.* using a hydrological model including the main physical processes governing water budget, and cryospheric dynamics, albeit simplified), to project forward hydrological cycle within the Maipo River until the end of the century. Our results are basically consistent with previous works, because they depict similar future changes, and statistically assessed trends therein, and further depict future evolution of ice cover in the area, and the most influencing climate drivers at the seasonal scale in the future. The present work has likely several limitations. Permafrost and rock glaciers in the area (Bodin, Pellicciotti & *alii*, 2015, Ranke & *alii*, 2015), were not explicitly modelled here, which may influence hydrological budget. Hydrological effect of permafrost, most notably played through the dynamics of the active layer (*e.g.* Kuchment & *alii*, 2000; Klene & *alii*, 2001) needs be studied *in situ*, and no such information is available for Maipo that we know of. A simplified melt model (degree day) for snow and ice was used here, when more complex methods are available, including enhanced (*e.g.* with solar radiation) temperature index models, or energy budget models (*e.g.* Pellicciotti & *alii*, 2008). However, degree day models applied at the daily scale often provide egregious depiction of melt for hydrological purposes (Ohmura, 2001; Bocchiola & *alii*, 2010; 2011; Soncini & *alii*, 2015). Also, more complex methods require large amount of data, including solar radiation, wind speed, air moisture, albedo, *etc.*, that are not normally available for long periods, and thus are normally feasible for studies limited in time (*e.g.* few melt seasons or so, Senese & *alii,* 2012). Also, for future projections of glacio-hydrological cycle as here, dependable projections of climate variables are required, which also would need downscaling against observed data, whenever available. Here, we simulated glacio-hydrological conditions for a long period, including the past three decades (1982-2013), and future projections until 2100 under 3 RCPs. Accordingly, use of a simplified temperature index model was more suitable. We lumped degree day of ice regardless of debris cover, mostly due to lack of knowledge about distributed debris thickness for glaciers in the area (as used *e.g.* in Bocchiola & *alii*, 2010; Soncini & *alii*, 2015; Minora & *alii*, in press, on the basis of extensive field campaigns). However, in the simplifying assumption that debris cover would not change largely in the future, possibly no large bias would be introduced. Some uncertainty may be laid within initial (2012) ice thickness estimates, provided by DGA (2012). In our catchment we mapped (referred to 2012) 341 km^2 of area covered with ice, with an estimated volume of 25.2 km^3 of water (*i.e.* ca. 74 m thickness on average). As a comparison, DGA (2011) for the whole Maipo catchment (larger than our catchment here) mapped ca. 388 km^2, with an estimated volume of ca. 37 km^3 (*i.e.* ca. 96 m in thickness on average), however largely variable depending upon the estimation method. In the future, some effort may be devoted to investigation of debris cover distribution for more accurate modelling of ice melt, and to investigation of the effect of rock glaciers, and permafrost, possibly adding variability to hydrological cycle. Variability of climate, and subsequent hydrology within projections from different models, normally affecting climate drivers and especially precipitation (*e.g.* Groppelli & *alii*, 2011b for Italy, Soncini & *alii*, 2015 for Karakoram, Palazzoli & *alii*, 2015 for Himalayas) may influence the results. Seasonal temperature patterns here are somewhat consistent between models, and consistent increase is seen with warmer RCPs. More variability is seen when it comes to precipitation. Here, on the long run (until 2100) decrease of precipitation is projected on average, and the more so with the warmest RCP8.5. Largest changes are foreseen during Fall and Winter, that are however the two wet seasons here (Tab. 3). Seasonal climate of Chile is sensitive to El Nino-Southern Oscillation ENSO events, falling out upon precipitation and hydrology (Cortés & *alii*, 2011). Pellicciotti & *alii* (2014) report that they used ECHM5 and Hadcm3 GCMs for projecting hydrology of the Juncal Norte glacier, given their capacity to represent ENSO events. ECHAM6 used here is an evolution of ECHAM5, so ideally being suitable for the purpose. Albeit no specific analysis was carried out here, we found that our GCM here depict somewhat acceptably seasonality of precipitation, and temperature in the area (*i.e.* compared *vs* ground based data, not shown), and even more so after downscaling. Accordingly, no large bias should be introduced here. Future steps may include sensitivity analysis of hydrological projections against climate projections, *e.g.* by way of synthetic simulation (*e.g.* stochastic realizations of climate patterns based upon GCM scenarios, *e.g.* Groppelli & *alii*, 2011b) beyond our scope in this manuscript, but still of interest. Even with uncertainty as entailed in projections of future climate and hydrology, our results here depict a consistent framework, in line with the present know how concerning future hydrology of the central Andes of Chile. Future deepening is required, and yet the main thread seems clear, and usable for adaptation measures for policy makers. Our study assesses potential impacts of climate change upon water resources from the central Andes of Chile, and most specifically in the Maipo catchment in Santiago region, under the most updated climate scenarios from AR5 of IPCC, until 2100, a topic much debated and of great interest for the scientific community and policy makers. During the three last decades Maipo underwent visible flow decrease at the yearly scale, and most notably in Spring and Summer, when water is utmost needed for irrigation. Decreasing trends are confirmed for the future in those seasons, most notably under the warmest RCPs towards mid century, when ice cover may be largely thinned, and evapotranspiration may draw large amount of moisture. Glacier cover would be increasingly thinned by rise of melting altitude, providing initially more water, but less water lately. Stream flows may increase at the expenses of ice cover during dry, increasingly warmer Fall and especially Winter, but the net effect will still be flow decrease *vs* historical series, especially under RCP8.5. Recent findings (Fuss & *alii*, 2014) indicate that late global temperature evolution, when compared against GCMs projections under IPCC AR5 launched mostly in 2006 (like in our GCM here), substantially overlap with the projected patterns according to RCP8.5, *i.e.* warming in the last decade proceeded according to the most pessimistic scenario. Seemingly therefore, if projections need be made now for the future, globally one may expect that the most credible of our scenarios here are those under RCP8.5. Notwithstanding the room for uncertainties in our approach, our results seem consistent, and credible, also in the face of the present literature for the area. Policy makers in Chile are therefore warned that climate change is acting, and will further act to decrease water availability in this region, and deplete ice cover therein, and adaptation needs be tackled soon enough.

REFERENCES

Barros V., Grimm A.M. & Doyle M.E. (2002) - *Relationship between temperature and circulation in southeastern South America and its influence from El Niño and La Niña events*. Journal of Meteorological Society of Japan, 80(1), 21-32.

Bocchiola D. (2007) - *Use of Scale Recursive Estimation for multisensor rainfall assimilation: a case study using data from TRMM (PR and TMI) and NEXRAD.* Advances in Water Resources, 30, 2354-2372.

Bocchiola D., Mihalcea C., Diolaiuti G., Mosconi B., Smiraglia C. & Rosso R. (2010) - *Flow prediction in high altitude ungauged catchments: a case study in the Italian Alps (Pantano Basin, Adamello Group)*. Advances in Water Resources, 33, 1224-1234.

Bocchiola D., Diolaiuti G., Soncini A., Mihalcea C., D'Agata C., Mayer C., Lambrecht A., Rosso R. & Smiraglia C. (2011) - *Prediction of future hydrological regimes in poorly gauged high altitude basins: the case study of the upper Indus, Pakistan*. Hydrology of Earth Systems Sciences, 15, 2059-2075.

Bocchiola D. & Diolaiuti G. (2013) - *Recent (1980-2009) evidence of climate change in the upper Karakoram, Pakistan*. Theoretical and Applied Climatology, 113(3-4), 611-641.

Bocchiola D. (2014) - *Long term (1921–2011) hydrological regime of Alpine catchments in Northern Italy*. Advances in Water Resources, 70, 51-64.

Bodin X., Rojas F. & Brenning A. (2011) - *Status and evolution of the cryosphere in the Andes of Santiago*. Geomorphology, 118, 453-64.

Bookhagen B. & Burbank D. W. (2006) - *Topography, relief, and TRMM-derived rainfall variations along the Himalaya*. Geophysical Research Letters, 33, L08405. doi: 10.1029/2006GL026037.

Bookhagen B. & Burbank D.W. (2010) - *Towards a complete Himalayan hydrologic budget: Thespatiotemporal distribution of snow melt and rainfall and their impact on river discharge*. Journal Geophysical Research. doi: 10.1029/2009jf001426.

Carrasco J. F., Casassa G. & Quintana J. (2005) - *Changes of the 0 C isotherm and the equilibrium line altitude in central Chile during the last quarter of the 20th century*. Hydrological Sciences Journal, 50 (6), 933-948.

Comisión Económica para América Latina y el Caribe (CEPAL) (2009) - *La Economía del Cambio Climático en Chile*. United Nations, Santiago, 88 pp.88.

Confortola G., Soncini A. & Bocchiola D. (2014) - *Climate change will affect water resources in the Alps: a case study in Italy.* Journal of Alpine Research, RGA/JAR, 100-3. http://rga.revues.org/2176.

Cortés G., Vargas X. & McPhee J. (2011). *Climatic sensitivity of streamflow timing in the extratropical western Andes Cordillera*. Journal of Hydrology, 2011, 405, 93-109.

Cortés G., Schaller S., Rojas M., Garcia L., Descalzi A., Vargas L. & McPhee J. (2012) - *Assessment of the current climate and expected climate changes in the Metropolitan Region of Santiago de Chile*. UFZ-Report 03/2012, Helmholtz Center for Environmental Research UFZ, Leipzig.

Cuffey K.M. & Paterson W. S. B. (2010) - *The Physics of Glaciers*,. 4th Edition, Academic Press, 704 pp.

DGA, Direccion General De Aguas, Gobierno de Chile, Unidad de Glaciología y Nieves (2011) - *Catastro, Exploración y Estudio de Glaciares en Chile Central*. Realizado por: Geoestudios Ltda, S.I.T. Nº 265.

DGA, Direccion General De Aguas, Gobierno de Chile, Unidad de Glaciología y Nieves (2012) - *Servicio De Consultoría: Plan De Accion Para La Conservación De Glaciares Ante El Cambio Climático*. Cooperación técnica no reembolsable ATN/OC-11996 –CH, Programa Plan de Acción para la Conservación de Glaciares ante Cambio Climático, DGA-BID, Sci. Coord. Diolaiuti, G., Informe Final.

Fuss S., Canadell J. G., Peters G.P., Tavoni M., Andrew R.M., Ciais P. & *alii* (2014) - *Betting on negative emissions*. Nature Climate Change, 4 (10), 850-853.

Garreaud R. & Aceituno P. (2001) - *Interannual rainfall variability over the South American Altiplano*, Journal of Climate, 14(12), 2779-2789.

Gent P. R. & twelve co-authors (2011) - *The Community Climate System Model Version 4*. Journal of Climate, 24, 4973-4991.

Groppelli B., Bocchiola D. & Rosso R. (2011a) - *Spatial downscaling of precipitation from GCMs for climate change projections using random cascades: A case study in Italy*. Water Resources Research, 47, W03519, doi: 10.1029/2010WR009437.

Groppelli B., Soncini A., Bocchiola D. & Rosso R. (2011b) - *Evaluation of future hydrological cycle under climate change scenarios in a mesoscale Alpine watershed of Italy.* NHESS, 11, 1769-1785. doi: 10.5194/nhess-11-1769-2011.

Hazeleger W. & eleven co-authors (2011) - *EC-Earth V2.2: description and validation of a new seamless earth system prediction model*. Climate Dynamics Journal , 39, 2611-2629.

Hock R. (1999) - *A distributed temperature-index ice- and snowmelt model including potential direct solar radiation.* Journal of Glaciology, 45(149).

Hock R. (2005) - *Glacier melt: a review of processes and their modelling*. Progress in Physical Geography 29, 3, 362-391.

IPCC (2013) - *Summary for Policymakers*. In: "Climate Change 2013: The Physical Science Basis". Contribution of Working Group I to the Fifth Assessment Report of the Intergovernmental Panel on Climate Change [Stocker T.F., Qin D., Plattner G.K., Tignor M., Allen S.K., Boschung J., Nauels A., Xia Y., Bex V. & Midgley P.M. (eds.)]. Cambridge University Press, Cambridge, United Kingdom and New York, NY, USA.

Izaurralde R.C., Williams J.R., McGill W.B., Rosenberg N.J. & Quiroga Jakas M.C. (2006) - *Simulating soil C dynamics with EPIC: Model description and testing against long-term data*. Ecological Modelling, 192, 3-4, 362-384.

Klene A.E., Nelson F.E., Shiklomanov N.I., Hinkel K.M. (2001) - *The N-Factor in Natural Landscapes: Variability of Air and Soil-Surface Temperatures, Kuparuk River Basin, Alaska, U.S.A*. Arctic, Antarctic and Alpine Research, 33(2), 140-148.

Krellenberg C. & Hansjürgens B. (2014) - *Climate Adaptation Santiago*. Springer-Verlag, Berlin Heidelberg, 221 pp.

Kuchment L.S., Gelfan A.N. & Demidov V.N. (2000) - *A distributed model of runoff generation in the permafrost regions*. Journal of Hydrology, 240(1-2), 1-22.

Masiokas M.H., Rivera A., Espizua L.E., Villalba R., Delgado S. & Aravena J.C. (2009) - *Glacier fluctuations in extratropical South America during the past 1000 years*. Palaeogeography, Palaeoclimatology, Palaeoecology, 281(3), 242-268.

Masiokas M.H., Villalba R., Luckman B.H., Le Quesne C., Aravena J.C. (2006) - *Snowpack Variations in the Central Andes of Argentina and Chile, 1951–2005: Large-Scale Atmospheric Influences and Implications for Water Resources in the Region.* Journal of Climate, 19, 6334-6352.

Mihalcea C., Mayer C., Diolaiuti G., Lambrecht A., & Smiraglia C. (2006) - *Ice ablation and meteorological conditions on the debris covered area of Baltoro Glacier, Karakoram (Pakistan)*. Annals of Glaciology, 43, 292-300.

Minora U., Bocchiola D., D'Agata C., Maragno D., Mayer C., Lambrecht A., Mosconi B., Vuillermoz E., Senese A., Compostella C., Smiraglia C. & Diolaiuti G. (2013) - *2001-2010 glacier changes in the Central Karakoram National Park: a contribution to evaluate the magnitude and rate of the Karakoram anomaly*. The Cryosphere Discussion, http://www.the-cryosphere-discuss.net/7/2891/2013/tcd-7-2891-2013.html.

Minora U.F., Senese A., Bocchiola D., Soncini A., D'Agata C., Ambrosini R., Mayer C., Lambrecht A., Vuillermoz E., Smiraglia C. & Diolaiuti G. (2015) - *A simple model to evaluate ice melt over the ablation area of glaciers in the Central Karakoram National Park, Pakistan*. Annals of Glaciology, 56(70), 202-216.

National Environmental Commission, Department of Climate Change (2010) - *National Climate Change Action Plan*. Teatinos 254/258, Santiago, Chile. http://www.mma.gob.cl/1304/articles-49744_Plan_02.pdf.

Oerlemans J. (2001) - *Glaciers and climate change*. A. A. Balkema Publishers, Brookfield, Vt.,148 pp.

Ohmura A. (2001) - *Physical basis for the temperature-based melt-index method*. Journal of Applied Meteorology, 40, 753-761.

Palazzoli I., Maskey S., Uhlenbrook S., Nana E. & Bocchiola D. (2015) - *Impact of prospective climate change on water resources and crop yields in the Indrawati basin, Nepal*. Agricultural Systems, 12, 143-157.

Parajka J. & Blöschl G. (2008a) - *The value of MODIS snow cover data in validating and calibrating conceptual hydrologic models*. Journal of Hydrology, 358, 240-258.

Parajka J. & Blöschl G. (2008b) - *Spatio-temporal combination of MODIS images-potential for snow cover mapping*. Water Resources Research, 44, 10.1029/2007WR006204.

Peel M. C., Finlayson B. L. & McMahon T. A. (2007) - *Updated world map of the Köppen-Geiger climate classification*. Hydrology and Earth System Sciences, 11, 1633-1644.

Pellicciotti F., Helbing J., Rivera A., Favier V., Corripio J., Araos J., & *alii* (2008) - *A study of the energy balance and melt regime on Juncal Norte Glacier, semi-arid Andes of central Chile, using melt models of different complexity*. Hydrological Process, 22, 3980-97.

Pellicciotti F., Ragettli S., Carenzo M. & McPhee J. (2014) - *Review: Changes of glaciers in the Andes of Chile and priorities for future work*. Science Tot. Environment, 493, 1197-1210.

Rabatel A. & 27 co-authors (2013) - *Current state of glaciers in the tropical Andes: a multi-century perspective on glacier evolution and climate change*. The Cryosphere, 7(1), 81-102.

Rabatel A., Castebrunet H., Favier V., Nicholson L., Kinnard C. (2011) - *Glacier changes in the Pascua-Lama region, Chilean Andes (29S): recent mass balance and 50 yr surface area variations*. The Cryosphere, 5, 1029–1041.

Ranke J.R., Bellisario A.C. & Ferrando F.A. (2015). *Classification of debris-covered glaciers and rock glaciers in the Andes of central Chile*. Geomorphology, 241(205), 98-121.

Rivera A., Acuña C., Casassa G. & Bown F. (2002) - *Use of remote sensing and field data to estimate the contribution of Chilean glaciers to the sea level rise*. Annals of Glaciology, 34, 367-72.

Rivera A., Casassa G., Acuña C., Lange H. (2000) - *Variaciones recientes de glaciares en Chile*. In Investigaciones Geograficas de Chile, 34, 29-60.

Rivera A., Bown F., Acuna C. & Ordenes F. (2009) - *I ghiacciai del Cile come indicatori dei cambiamenti climatici / Chilean glaciers as indicators of climatic change*. Terra Glacialis Edizione speciale / Special issue "Mountain glaciers and climate changes in the last century". http://repositorio.uchile.cl/bitstream/handle/2250/117817/113801_C11_rivera-italia.pdf?sequence=1.

Rosso R. (1984) - *Nash model relation to Horton order ratios*. Water Resources Research, 20(7), 914-920.

Senese A., Diolaiuti G., Mihalcea C. & Smiraglia C. (2012). *Energy and Mass Balance of Forni Glacier (Stelvio National Park, Italian Alps) from a Four-Year Meteorological Data Record*. Arctic, Antarctic and Alpine Research, 44(1),122-134.

Singh P., Kumar N., Arora M. (2000). *Degree–day factors for snow and ice for Dokriani Glacier, Garhwal Himalayas*. Journal of Hydrology, 235(1),1-11.

Soncini A., Bocchiola D., Confortola G., Bianchi A., Rosso R., Mayer C., Lambrecht A., Palazzi E., Smiraglia C. & Diolaiuti G. (2015) - *Future hydrological regimes in the upper Indus basin: a case study from a high altitude glacierized catchment*. Journal of Hydrometeorology, 16(1), 306-326.

Soncini A. & Bocchiola D. (2011) - *Assessment of future snowfall regimes within the Italian Alps using general circulation models*. Cold Regions Science and Technology, 68(3), 113-123.

Stevens B. & other 16 co-authors (2013) - *Atmospheric component of the MPI-M Earth System Model: ECHAM6*. Journal of Advances in Modeling Earth System, 5, 1-27.

Urrutia R. & Vuille M. (2009) - *Climate change projections for the tropical Andes using a regional climate model: Temperature and precipitation simulations for the end of the 21st century*. Journal of Geophysical Research, 114(D2), 2156-2202.

Wallinga J. & van de Wal R.S.W. (1998) - *Sensitivity of Rhonegletscher, Switzerland, to climate change: experiments with a one-dimensional flowline model*. Journal of Glaciology, 44(147), 383-393.

(Ms. received 30 March 2014; accepted 30 September 2015)